[3]Miller, C.G., "Measured Pressure Distributions, Aerodynamic Coefficients and Shock Shapes on Blunt Bodies of Revolution at Incidence in Mach 6 Air and CF_4 and Mach 10 Air," NASA TM 84489, Sept. 1982.

[4]Midden, R.E. and Miller, C.G., "Description and Preliminary Calibration Results for the Langley Hypersonic CF_4 Tunnel," NASA TM 78800, 1978.

[5]Foust, J.W., "Entry Heat Transfer Tests of the 0.006-Scale Space Shuttle (−147B) Orbiter Model (50-0) in the Langley Research Center Freon Tunnel at Mach 6 (OH45)," NASA CR-141,527, Dec. 1975.

[6]Miller, C.G. III, "Comparison of Thin-Film Resistance Heat-Transfer Gages with Thin-Skin Transient Calorimeter Gages in Conventional Hypersonic Wind Tunnels," NASA TM 83197, Dec. 1981.

[7]Zoby, E.V., "Approximate Heating Analysis for the Windward-Symmetry Plane of Shuttle-Like Bodies at Large Angle of Attack," *Thermophysics of Atmospheric Entry: AIAA Progress in Astronautics and Aeronautics,* Vol. 82, edited by T.E. Horton, AIAA, New York, 1982, pp. 229-247.

[8]Hamilton, H.H., "Approximate Method of Predicting Heating on the Windward Side of Space Shuttle Orbiter and Comparisons with Flight Data," AIAA Paper 82-0823, June 1982.

[9]Herrera, B.J., "Results From a Convective Heat Transfer Rate Distribution Test on a 0.0175 Scale Model (22-0) of the Rockwell International Vehicle 4 Space Shuttle Configuration in the AEDC-VKF Tunnel B (OH498)," Vol. 1 of 2, NASA CR-147,626, 1976.

[10]Griffith, B.J., Majors, B.M., and Adams, J.C., "Blunt Body Boundary-Layer Parameters Including Shock Swallowing Effects," *Thermophysics of Atmospheric Entry: AIAA Progress in Astronautics and Aeronautics,* Vol. 82, edited by T.E. Horton, AIAA, New York, 1982, pp. 90-111.

A Novel Concept for Reducing Thermal Contact Resistance

R.S. Cook,* K.H. Token,† and R.L. Calkins‡
McDonnell Aircraft Company,
St. Louis, Missouri

Introduction

MECHANICAL joints, which must be opened periodically for equipment inspection or maintenance, are encountered in many equipment cooling designs, particularly those for electronic equipment. The thermal contact resistance at interfaces in electronics either elevates operating temperatures, which degrades component reliability, or increases coolant demand, which increases cooling system size and power requirements.

A novel concept for reducing thermal contact resistance has been identified and tested. It does not require high contact pressure or smooth surface finishes for good thermal performance, and it does not inhibit joint assembly or disassembly.

The Improved Thermal Joint Concept

The key feature of this new concept is the incorporation of a low-melting-point metallic alloy in an interstitial material. At room temperature the alloy is in the solid state to aid assembly and disassembly of the joint. The selected alloy has a melting point below the operating temperature of the joint. During operation, heat transferred to the joint raises the interface temperature, causing the alloy to change phase to the liquid state. The liquid metal then flows freely to fill the interstitial voids, as indicated in Fig. 1.

The improved thermal joint has several noteworthy characteristics. When the alloy is liquid it provides a continuous metallic heat-transfer path, which significantly reduces contact resistance. Since the alloy is liquid at operating temperatures, high contact pressure is not required to force the interstitial material into voids. Joint disassembly after cool down and solidification of the alloy is accomplished easily since many low-melting-point alloys will not adhere strongly to metallic or nonmetallic surfaces unless they are exceptionally clean and free of oxides. Also, a number of candidate alloys are available (see Ref. 1 for a list of 190 alloys with melting points ranging from −54 to 590°F).

Improved Thermal Joint Embodiments

Three embodiments have been investigated. The first (Fig. 2) employs a porous metallic structure (carrier) to contain the liquid metal alloy. Capillarity prevents the liquid metal from flowing out of the interstice during inertial or gravitational accelerations. This embodiment is referred to as the "porous carrier."

The second embodiment (Fig. 2) consists of a thin sheet of solid carrier material (e.g., copper or copper-plated aluminum) coated on both sides with a thin layer of the low-melting-point alloy, which is inserted between the joining surfaces. At operating temperature the alloy liquifies and fills the interstitial voids. Following cool down and solidification, the alloy is retained on the carrier by a strong bond. The bond with the surface material is weak, however, allowing easy separation of the joint and removal of the alloy-coated carrier. This embodiment is referred to as the "solid carrier." For those applications where a separable carrier is undesirable, the carrier material (e.g., electroplated copper) can be applied directly to one of the joining surfaces.

The third embodiment (Fig. 2) consists of a thin sheet of low-melting-point alloy which is inserted between the joining surfaces. When heated, the alloy liquifies and fills the interstitial voids. The weak affinity between the alloy and the surface material allows easy separation of the cold joint. Thermal performance is restored by inserting a new sheet of alloy between the joining surfaces during reassembly. This embodiment is referred to as the "alloy" joint.

Development Test Program

A test program was conducted to verify the improved thermal joint concept and develop the most promising embodiment. Preliminary tests established approximate thermal contact resistance values for each embodiment in contact with 6061-T6 aluminum surfaces, frequently encountered in electronic packaging. Static measurements based on the thermal comparator method indicated significantly less contact resistance than for a reference bare aluminum joint. Prototypes were accelerated on a centrifuge to evaluate each for loss of liquid metal from the interstice. Additional static

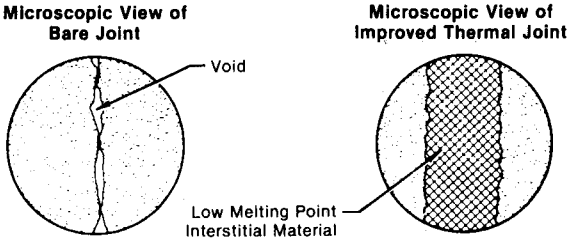

Fig. 1 Improved thermal joint concept.

Presented as Paper 82-0886 at the AIAA/ASME 3rd Joint Thermophysics, Fluids, Plasma and Heat Transfer Conference, St. Louis, Mo., June 7-11, 1982; submitted June 14, 1982; revision received March 31, 1983.

*Technical Specialist, Propulsion and Thermodynamics Department, Engineering Technology Division.

†Branch Chief, Propulsion and Thermodynamics Department, Engineering Technology Division. Member AIAA.

‡Senior Engineer, Materials Laboratory, Flight and Laboratory Development Division.

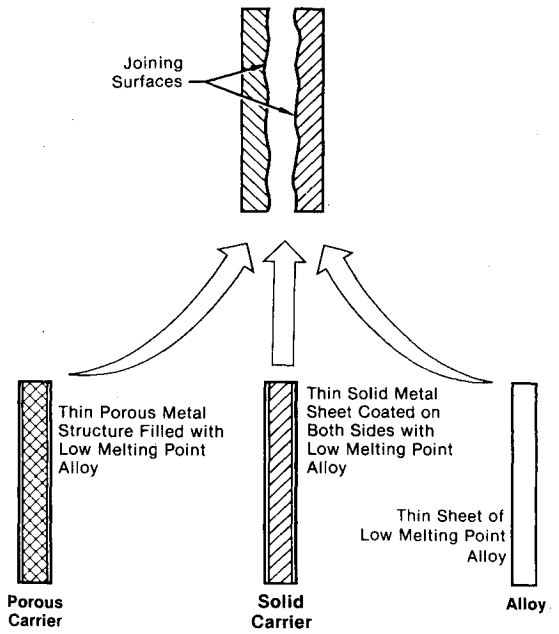

Fig. 2 Basic improved thermal joint embodiments.

tests were conducted to determine contact resistance values as a function of contact pressure and surface roughness.

Centrifuge Tests

Each embodiment was subjected to inertial accelerations on a centrifuge. The interstitial material was inserted between aluminum surfaces with a roughness of 60 μin. rms. Contact pressure was 17 psi. The test results indicated that a loss of liquid metal from the interstice occurred between 1 and 2g for all three embodiments when accelerations were applied in the plane of the joint. These results were unacceptable for airborne equipment. A solution based on a modification of the solid carrier was identified.

The Segmented Surface

For the solid carrier, retention of liquid metal alloy in the interstice during acceleration is limited by the continuous length of alloy-coated surface in the direction of applied accelerations. This surface dimension determines the head of liquid metal which must be supported during acceleration by capillary forces in the joint. Acceleration capability can be increased by segmenting the interstitial material surfaces into smaller alloy-coated areas, separated by narrow gaps which are not wetted by the liquid metal. An example of this approach is shown in Fig. 3. The small alloy-coated square cells reduce the hydrostatic head of liquid metal which must be supported by capillary forces.

Segmented Surface Validation

A multicell segmented surface was designed, fabricated, and tested on the centrifuge. Cell and gap size were selected to meet a 10g aircraft acceleration requirement. Contact resistance was determined by the thermal comparator method. The thermal comparator was mounted on the centrifuge so that the accelerations were applied in the plane of the joint.

Three specimens were tested. Each was inserted between aluminum surfaces. Surface roughness was approximately 60 μin. rms, and contact pressure was nominally 30 psi. The test results indicated that accelerations up to 10g had no significant influence on thermal resistance. Visual inspection of the test specimens following the 10g acceleration confirmed that the liquid metal was retained in the joint.

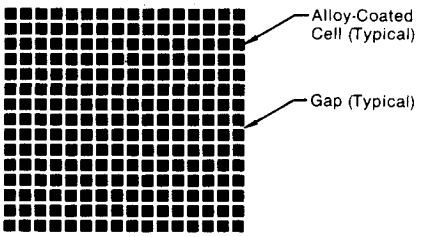

Fig. 3 Example of segmented surface.

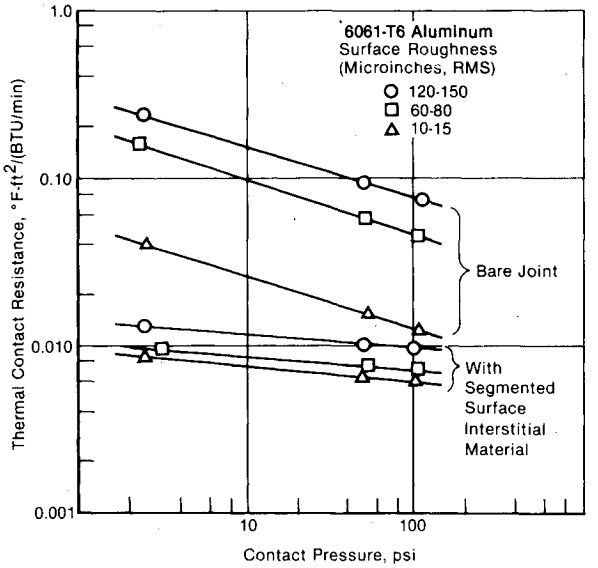

Fig. 4 Static thermal resistance test results (1 atm).

Static Thermal Resistance Tests

A series of tests was conducted to determine the effect of surface roughness and contact pressure on the thermal resistance of the segmented surface. The surface pattern consisted of 0.125 in. square cells separated by 0.030 in. gaps.

The test samples consisted of the segmented surface interstitial material located between 6061-T6 aluminum, with mating surface roughness of 120-150, 60-80, and 10-15 μin. rms. The average flatness of each mating surface was $\pm$0.0002 in.

Reference bare joint thermal resistance data were obtained for nominal contact pressures of 100, 50, and 3 psi. After each bare joint run, a segmented surface specimen was installed between the aluminum surfaces and the test was repeated. Figure 4 summarizes the thermal resistance test results for the bare joint and the segmented surface interstitial material. As anticipated, the bare joint contact resistance decreases with increasing contact pressure and reduced surface roughness. The results shown for the bare joint are in good agreement with other published data for aluminum-to-aluminum joints at 1 atm ambient pressure.[2] The thermal performance of the segmented surface specimens was found to be relatively insensitive to contact pressure and surface finish over the range tested. A somewhat conservative value of 0.01°F-ft^2/Btu/min may be used for contact resistance with the segmented surface interstitial material. This is a significant reduction in thermal resistance compared to the bare joint, particularly for moderate values of contact pressure (50 psi) and surface roughness (60-80 μin. rms).

Development Status

The improved thermal joint has been reduced to practice, and U.S. patents are pending. Because of the promising results obtained to date, development of the segmented

surface is continuing. Interstitial material fabrication techniques are being evaluated to identify improvements in quality and producibility. Additional tests are planned to evaluate the effects of environmental conditions (temperature, ambient pressure, shock, vibration, etc.) on the interstitial material and its thermal performance.

Conclusions

The improved thermal joint can reduce contact resistance at metal-to-metal interfaces by up to a factor of 10. Through proper selection of materials and surface treatment, the joining surfaces may be separated easily after solidification of the low-melting-point alloy. The segmented surface can also provide low thermal resistance during high inertial accelerations. While this technology is being developed to improve thermal control of airborne electronics, it potentially can be applied to many interface heat-transfer problems where low contact resistance and ease of joint disassembly are desired.

References

[1]Mantell, C.L., ed., *Engineering Materials Handbook,* McGraw-Hill, New York, 1958.

[2]Barzelay, M.E., Tong, K.N., and Holloway, G.F., "Effect of Pressure on Thermal Conductance of Contact Joints," NACA TN 3295, May 1955.

Despin of a Liquid-Filled Cylinder Caused by Coning

Roger F. Gans*
ARRADCOM-U.S. Army Ballistic Research Laboratory, Aberdeen Proving Ground, Maryland

D'AMICO and Miller[1] reported a series of despin experiments using a laboratory spin fixture undertaken in an effort to understand the unstable flight of liquid-filled projectiles at "high viscosity" (in the sense that the Ekman number, $E=\nu/\omega a^2$, is larger than 10^{-3}) where ν, ω, and a denote the liquid kinematic viscosity, projectile spin rate, and cavity radius. These were compared to flight data, and qualitative agreement was shown, in the limited sense that stable flights corresponded to low despin rates and unstable flights to high despin rates. No attempt to understand the mechanism was made in that report. This Note will demonstrate qualitative agreement with a mechanism drawn from the linear theory of forced coning motion.

The experiments were performed in a cylindrical container which had an inner radius $a=60.3$ mm and half height $c=258.7$ mm. The container was filled completely with a liquid of a given viscosity and spun up to 66.67 Hz about its symmetry axis, inclined 20 deg to the vertical. After the liquid-container system had come to equilibrium, the spin drive was turned off and the spin axis forced to cone at 8.33 Hz about the vertical. The spin rate was recorded as the container spun down from 66.67 to 33.33 Hz. The data were reasonably well represented by a simple exponential decay, and the decay constants were measured. The previously measured frictional decay was subtracted, and the resulting net liquid-caused decay was converted to a (despin) moment about the spin axis.

The data can be interpreted in terms of the response of a contained rotating liquid to coning motion of its container. Let Ω denote the coning rate, α the coning angle, and $\epsilon=(\Omega/\omega)\sin\alpha$. If ϵ and E (defined earlier) are both small compared to unity, the equations governing the motion of the fluid can be solved by linearizing about a state of solid rotation and applying a boundary-layer approximation. The linear response is of the order ϵ unless the coning rate is comparable to the frequency of one of the free oscillations of the rotating liquid. In that case, the response is dominated by the resonant mode, and its amplitude is of order ϵ divided by the sum of e $(=E^{1/2})$ and a number representing the nearness to the resonant geometry.[2]

The resonant eigenfunction for the pressure is given by

$$J_l(jr)\sin(kz)\cos(\phi+\beta)$$

where r, ϕ, z are the usual cylindrical coordinates, J_l the first-order Bessel function of the first kind, and j and k constants such that

$$\cos(kc/a)=0; \qquad sjJ_l'(j)+2J_l(j)=0$$

and $j^2=X^2k^2$, where

$$X^2=(4-s^2)/s^2; \qquad s=1-\Omega/\omega$$

prime denotes the derivative with respect to the argument, and β is a phase angle which depends on viscosity.

The linear response so calculated is periodic in the azimuthal angle (measured with respect to the spin axis), and so it cannot contribute to torque about the spin axis. Thus, the despin torque must arise from the flow driven by nonlinear interactions which leads to axisymmetric torques. (In principle the linear calculation could be extended to find these torques. In practice that is an extremely intricate calculation which is well beyond the scope of this Note.) It is possible to show[3] that the despin torque will be dominated by the viscous shear stress in the boundary layer which has a thickness proportional to $(\nu/\omega)^{1/2}$ Thus, the despin torque can be written symbolically as

$$\text{torque} \propto (\text{viscosity})(\text{linear amplitude})^2 \div \text{boundary-layer thickness})$$

The container used in the despin experiments just discussed has a length-to-diameter ratio of 4.291, and there are two resonances which may be important. One has a radial wavenumber of unity and an axial half-wave number of two. The other has a radial wave number of two and an axial half-wavenumber of four. The critical s and j for these modes are 0.7325281 and 2.899531 for the former and 0.840394 and 5.750889 for the latter. Thus, the critical coning rates are in the range of 1/6 to 1/4 of the rotational rate, so the despin experiments described can be expected to excite one or the other of these modes.

Interpretation of the experiment is complicated by the change in spin rate during the experiment. This leads to a continuous change in the expected critical coning rate, and a state of flow different from that postulated by the theory; i.e., the fluid cannot respond instantaneously to the change in the spin rate of its container and so is not well-modeled by a simple departure from solid rotation. In addition, it is well-known that a liquid which is spinning more rapidly than its container is likely to be centrifugally unstable.[4]

However, the observed rate of decay of spin is essentially constant at spin rates above about 17 Hz, and the ideas discussed earlier provide an impressive correlation with the data. Figure 1 shows the data from Ref. 1 plotted against the

Submitted March 4, 1983; revision received July 1, 1983. This paper is declared a work of the U.S. Government and therefore is in the public domain.

*Associate Professor of Mechanical Engineering, University of Rochester, Rochester, N.Y. (on leave).